A PCA-based method to select the number and the body location of piezoresistive sensors in a wearable system for respiratory monitoring

Luigi Raiano[1†], *Student Member, IEEE*, Joshua Di Tocco[2†], *Student Member, IEEE*, Carlo Massaroni[2], *Member, IEEE*, Giovanni Di Pino[1], Emiliano Schena[2], *Senior Member, IEEE* and Domenico Formica[1], *Senior Member, IEEE*

***Abstract*— This work aims at selecting the number and the body location of piezoresistive sensors to instrument wearable systems for respiratory rate (RR) estimation. We tested a novel method based on Principal Component Analysis on 10 healthy male subjects, who were asked to perform six trials on a treadmill (at rest, during walking and low speed running). We monitored RR using both a smart garment composed of six piezoresistive sensors and a flowmeter, used as reference signal. On the basis of the results, we propose the following guidelines: i) breathing assessment at rest requires one sensor, placed on the lower thorax; ii) low speed walking assessment requires three sensors, placed on upper thorax, lower thorax and abdomen; iii) high speed walking and running assessment requires a four-sensor configuration (one sensor placed on the upper thorax, one on the lower thorax and two on the abdomen); iv) an effective assessment can be performed at all speeds using the above-mentioned four-sensor configuration, denoted as General Purpose Configuration.**

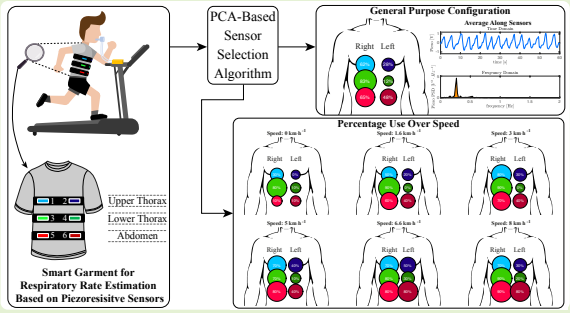

***Index Terms*— Breathing activity monitoring, Piezoresistive sensors, Respiratory monitoring, Smart garment, Strain sensors, Wearable systems.**

I. Introduction

CONTINUOUS monitoring of physiological activities such as breathing, blood pressure, heart activities and body temperature, has gained momentum in a variety of applications [1].

Among others, the knowledge of respiratory rate (RR) may be beneficial to assess the patients' status since it is sensitive to environmental and physiological stressors [2]. RR can be monitored by different techniques that can be classified into two main categories: contact-based techniques and contactless ones [3]–[7]. In this arena, several wearable systems based on the detection of the rib cage deformation have been developed [4]. There are different approaches to design this kind of wearables (*i.e.* resistive [8], capacitive [9], inductive [10], fiber optic [11]–[13] and humidity sensors [14]) and piezoresistive sensing elements have gained increasing attention due to their characteristics of comfortability, wearability, ease of use and reduced costs [4], [15]–[18]. Indeed, the use of piezoresistive sensors enables the design of highly integrated flexible systems, where the sensor structure fulfils the role both of support material and sensitive element itself, differently to classical strain gauges which can only measure the deformation applied on it [19]. Such characteristics allow obtaining compact sensors that can be easily integrated, sewed or even directly embedded, within clothes (*e.g.,* elastic bands or t-shirts) [4]. Another advantage of using piezoresistive sensors to design wearable smart-textiles for monitoring RR is the relative simplicity of the conditioning electronic needed to let them properly work, even characterized by a very low power consumption [20]. All the above-mentioned characteristics make this technology an affordable solution for estimating the RR in unstructured environments.

The main drawback of using piezoresistive sensors for RR monitoring consists in their sensitivity also on breathing-unrelated movements. In this regard, the problem of data clean-

This work was partially funded by SENSE-RISC project (ID10/2018) funded by National Institute for Insurance against Accidents at Work (INAIL) and H2020/ICT European project CONBOTS ("CONnected through roBOTS: physically coupling humans to boost handwriting and music learning", Grant Agreement no. 871803, call topic ICT-09-2019-2020).

[1]NeXT: Neurophysiology and Neuroengineering of Human-Technology Interaction Research Unit, Università Campus Bio-Medico di Roma, Rome, Italy {l.raiano, g.dipino, d.formica}@unicampus.it

[2]Unit of Measurements, Università Campus Bio-Medico di Roma, Rome, Italy {j.ditocco, c.massaroni, e.schena}@unicampus.it

†These authors contributed equally to this work.

ing has been widely studied so far. Indeed, when attempting to continuously monitor RR during physical activities, e.g., walking or running, its correct assessment is hindered by the presence of motion artifacts [21]–[23]. Filtering techniques [21], [24]–[26] or processing methods based on Independent Component Analysis have been proposed to reduce the presence of such artifacts [27], [28]. Nevertheless, recent studies have demonstrated that the use of a band-pass filter from 0.05 Hz to 2 Hz allows to properly estimate RR [29], [30].

On the other hand, a little is known concerning the optimal number of sensors to be employed and their appropriate body location, both at rest and during physical activity [31]. In order to fill such a gap, in this work we provide a systematic approach to define the number of piezoresistive sensors and their body location, which would allow implementing a robust estimation of the RR at rest, during walking and running. Our approach is based on Principal Component Analysis (PCA) and we tested the results obtained estimating both average and breath-by-breath RR.

The outcome of this study may help to develop optimized instrumented wearable devices for RR monitoring and to implement dedicated algorithms to continuously and reliably monitor RR at rest and during physical activity.

II. Smart Garment

The proposed smart garment is composed of three elastic bands embedding two piezoresistive sensors each. The bands are equipped with Velcro strips to adapt the system to the subjects' anthropometry. The bands allow allocating the sensors avoiding both any contact with the users' skin and issues related to the presence of sweating. Each sensor is obtained from an A4 sheet of silver-plated knitted fabric (STATEX Shieldex® Technik-tex P130+B [32]), composed of 78 % Polyamide and 22 % Elastomer. They are cut in a rectangular shape (L×W: 50 mm × 10 mm) and hand sewed on the bands as represented in Fig. 1A.

The choice of six elements placed on three bands is threefold:

- to allow properly monitoring the movements of the rib cage, which during the respiratory activity can be divided into three main areas: i) pulmonary Rib Cage, ii) abdominal Rib Cage and iii) Abdomen [33];
- to increase the robustness of the system if one element damages;
- to compare right side and left side of the torso during walking/running characteristics.

Moreover, the use of a multi-sensor system could provide information on which sensors are mostly used in a certain physical activity (i.e., standing, walking and running), and it will also give a clearer understanding of which part of the rib cage is mostly involved in each activity.

The smart garment (composed of N = 6 sensors) allows recording the respiratory signals associated to the strain provided by the cyclic expansion and contraction of the rib cage to the elastic bands, on which the sensors are fixed. To retrieve the respiratory signal a custom printed circuit board (PCB) has been developed. It embeds Wheatstone bridges to transduce the resistance variation (i.e., the output of the piezoresistive sensors) into voltage variation, instrumentation amplifiers, an Analog to Digital Converter (ADC), and a Bluetooth module to transmit the converted data to a laptop running a custom algorithm in MATLAB environment.

III. Experimental Setup

We carried out a series of experiments employing the setup presented in Fig. 1 B. It consists of:

- a treadmill (Walker-View by TecnoBody s.r.l), used to set and maintain the desired walking and running speed of the experimental trials for 60 s;
- a reference sensor (i.e., the flowmeter SpiroQuant P by EnviteC, Honeywell [34])]). The breathing pattern was recorded by measuring the airflow at the level of the mouth using a mouthpiece. The flowmeter converts the flowrate into a pressure drop which is measured by a differential pressure sensor (163PC01D36 by Honeywell) between two static taps. The reference respiratory data were collected using a data acquisition board (DAQ NI USB6002 by National Instrument) via a custom Virtual Instrument in LabView environment;
- a smart garment, used to retrieve the respiratory information in the three compartmental areas, providing six respiratory signals.

After the approval of the ethical committee, we enrolled ten male healthy volunteers (N_{subjs} = 10). Additional information on the population is reported in the supplementary material.

Subjects were asked to wear the smart garment and the mouthpiece, and to perform six different trials on the treadmill: one trial at rest (standing in absence of movements, *i.e.*, speed equal to 0 km·h^{-1}), four walking trials at 1.6 km·h^{-1}, 3.0 km·h^{-1}, 5.0 km·h^{-1}, 6.6 km·h^{-1}, and a low speed running trial at 8.0 km·h^{-1}. All trials have been performed indoor, with the room temperature controlled and set to 25°C.

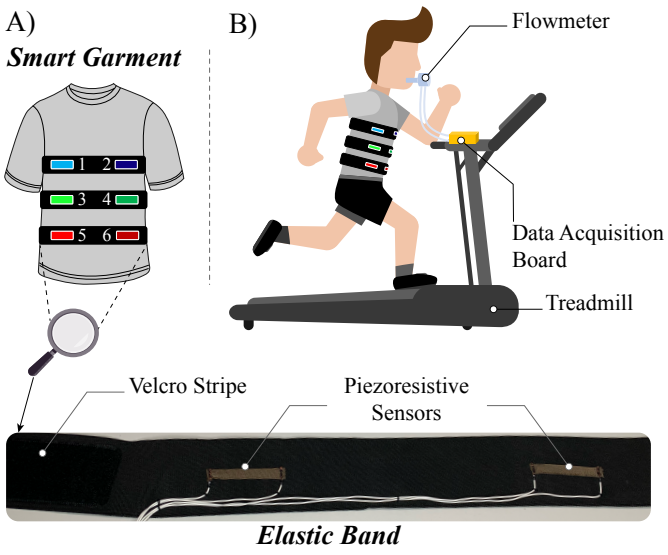

Fig. 1. A) Overview of the smart garment used. B) Schematic representation of the experimental setup.

IV. Proposed Algorithm for Sensor Selection

One of the most used technique to deal with dimensionality reduction is the Principal Component Analysis (*PCA*). It allows representing the observations recorded in a set of new orthogonal variables, defined as Principal Components (*PC*s), [35].

Let $\boldsymbol{X}$ be the $M \times N$ matrix of the centered recorded observations, denoting M the number of samples and N the number of sensors used, the *PC*s can be computed as follows:

$$\boldsymbol{PC} = \boldsymbol{X}\,\boldsymbol{U}. \tag{1}$$

In (1), $\boldsymbol{PC}$ is a $M \times P$ matrix, denoting P the number of *PC*s (which can be at most equal to N), while $\boldsymbol{U}$ denotes the $N \times P$ coefficient matrix which maps the contribution of each observed sensor to the *PC*s [36]. Considering the *PC*s sorted in a decreasing order in terms of variance explained of the recorded observations, it is possible to select a subset of *PC*s (*i.e.* $p < P$) to explain a part of the total variance. This is defined as *accounted variance* and typically expressed as a percentage of the total one. The higher the accounted variance desired, the higher the number of *PC*s needed [36].

Our method aims both at minimizing the number of piezoresistive sensors and optimizing their body location. Two subsequent sensor selection stages are performed:

- to retain the first p components needed to get an accounted variance equal to 95% and exclude the sensors which have a representation in the selected components below 15% (considered as noisy sensors with low influence on the explained variance; see Supplementary Materials for the justification of these thresholds);
- to remove from the remaining sensors all those which provide redundant information. We considered as redundant sensors the pairs with a correlation above 80%; then, for each pair we excluded the sensor with the lowest weight in the selected *PC*s. We opted to use a threshold of 80% since it refers to a *high similarity* between the signals correlated [37].

The complete description of the proposed algorithm implemented for each subject and each speed, is the following:

1) to band-pass filter the input data from 0.05 Hz to 2 Hz; this filter has been implemented in MATLAB^{TM} through its embedded function "*filtfilt*". We selected 0.05 Hz as low cut-off frequency in order to discard very slow signal variations from the recorded data; conversely, we selected 2 Hz as high cut-off frequency, since the activity of interest for this application (*i.e.*, breathing) is hardly above 1.5 Hz, and we aimed to filter out components not relevant for our application while avoiding to discard any useful information recorded by the sensors [26];
2) to perform a centering operation, so that the mean of each signal is equal to zero [35];
3) to run the PCA algorithm, implemented in MATLAB^{TM} through its embedded function "*pca*";
4) to select p in order to get an accounted variance equal to the 95%;
5) to compute the weight of the i-th sensor (w_i) along the p *PC*s as follows:

$$\begin{cases} w_i = \frac{z_i}{\sum_{i=1}^{N} z_i} \cdot 100 \quad [\%] \\ z_i = \sum_{k=1}^{p} |u_{i,k}|. \end{cases} \tag{2}$$

In (2) the term $|u_{i,k}|$ denotes the absolute value of the element of the matrix $\boldsymbol{U}$ related to the i-th sensor and the k-th PC, *i.e.* the weight of the i-th sensor for the k-th PC, according to (1);
6) to discard all those sensors whose w_i is lower than $15\,\%$;
7) to run a linear correlation between all sensor pairs; in case of a Pearson's correlation coefficient (ρ) higher than 0.8 the two sensors are marked as a highly correlated pair [37];
8) to discard the redundant sensors; for each *highly correlated pair*, the sensor with the lowest weight on *PCs* is marked as redundant and then discarded;

The flowchart of the proposed method is presented in Fig. 2.

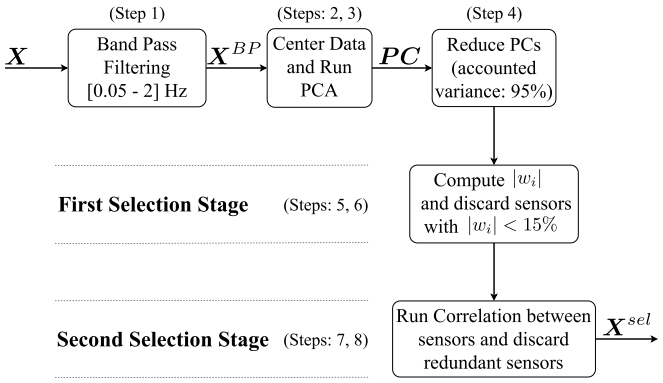

Fig. 2. Flowchart of the proposed method for selecting non-redundant piezoresistive sensors in breathing activity monitoring. The symbol $\boldsymbol{X}$ denotes the input piezoresistive signals; $\boldsymbol{X^{BP}}$ denotes the input data band-pass filtered; $\boldsymbol{PC}$ represents the principal components estimated; $\boldsymbol{X^{sel}}$ denotes the selected piezoresistive signals, *i.e.* the output of the method.

V. Data Analysis

The aim of the data analysis is two-fold: i) to optimize the number of sensors and their body location at each speed and ii) to assess the feasibility of the proposed selection method for estimating RR. Moreover, we compared the results of the proposed method with those obtained using the method proposed by Di Tocco et al. [26] (selection of four piezoresistive sensors out of six by discarding the two sensors showing the highest and the lowest amplitude of the power spectral density, PSD). Besides indicating the optimal set of sensors for each speed and each tested subject, we also assessed the performance of a single configuration including the sensors that in average have been mostly selected in all subjects and in all trials. This further step allows validating the performance of a general purpose smart garment, not optimized neither for a single speed nor on a single subject, rather characterized by a reduced set of sensors.

Denoting SG the signals related to the smart garment (*i.e.*, the specific sensor configuration), we adopted the following notation:

- *Selected Sensors* ($SG \equiv \boldsymbol{X}^{sel}$): piezoresistive signals processed through the proposed selection method, *i.e.*, all those sensors kept at the end of the two selection stages;
- Method proposed by Di Tocco et al. ($SG \equiv \boldsymbol{X}^{DT}$): piezoresistive signals processed using the selection method presented in [26] and used as reference for comparing our new approach;
- *General Purpose Configuration* ($SG \equiv \boldsymbol{X}^{GPC}$): configuration of the smart garment composed of the four most used sensors among all subjects and trials (see Section VI-A)

A. Sensor Selection

The percentage use of the i-th sensor (with $i = \{S_1, S_2, S_3, S_4, S_5, S_6\}$) at j-th trial speed ($j = \{0$ km·h^{-1}, 1.6 km·h^{-1}, 3.0 km·h^{-1}, 5.0 km·h^{-1}, 6.6 km·h^{-1}, 8.0 km·h$^{-1}\}$) is defined as the sum of the number of uses (${}^{j}\zeta_{i,h}$) of the i-th sensor at j-th speed along all subjects:

$$ {}^{j}\Omega_i = \sum_{h=1}^{N_{subjs}} {}^{j}\zeta_{i,h} \cdot \frac{100}{N_{subjs}} \, [\%] \, . \tag{3} $$

In addition, we also computed the mean number of the sensors selected by the proposed method at each speed, averaged along all subjects.

Finally, the average percentage use of the i-th sensor (Ω_i) is the average of ${}^{j}\Omega_i$ along the six trail speeds.

B. Performance Assessment

We assessed the performance in estimating RR, considering both the RR averaged in the whole trial and considering breath-by-breath. Specifically we compared both $\boldsymbol{X}^{sel}$ and $\boldsymbol{X}^{GPC}$ with respect to $\boldsymbol{X}^{DT}$. In this regard, we used the following further symbols:

- φ: reference flowmeter signal;
- l: number of piezoresistive sensors considered; $l = 4$ both for $\boldsymbol{X}^{DT}$ [26] and $\boldsymbol{X}^{GPC}$, while concerning $\boldsymbol{X}^{sel}$, the actual value of l depends on the number of sensors selected.

Despite the signal artifact due to breathing-unrelated movements can affect the signals recorded by the piezoresistive sensors, it does not hinder a correct estimation of RR as already shown in [29], [30]. Such studies showed that the main body motion artifact is related to the torso rotation during walking or running and it is characterized by a specific contribution in the frequency domain (i.e., ∼1.5 Hz) clearly separated from the one of the RR (i.e., typically lower than 1 Hz) [38].

1) Average RR Estimation: The frequency domain allowed us to determine the performance in estimating the average RR during each trial. Specifically, we compared the spectrum of $\boldsymbol{X}^{sel}$, $\boldsymbol{X}^{DT}$ and $\boldsymbol{X}^{GPC}$ with the one of φ for each trial speed. In this regard, we considered the frequency error ($\tilde{F}_h^{SG}$) between the frequency corresponding to the maximal peak found in the PSD of φ (F_h^{φ}) and the frequency corresponding to the maximal peak found in the average PSD of piezoresistive signals along the l sensors (F_h^{SG}) on h-th subject:

$$ \tilde{F}_h^{SG} = F_h^{\varphi} - F_h^{SG} \quad [bpm]. \tag{4} $$

In (4) the symbol "bpm" refers to *breath per minutes*; the average of $\tilde{F}_h^{SG}$ along all subjects is denoted with $\tilde{F}^{SG}$;

2) Breath-by-Breath Assessment: The time domain assessment allowed us to perform a breath-by-breath analysis. Firstly, we calculated the breath duration $T_R[n]$ between two consecutive inspiratory peaks both for φ and SG using custom parameters in a peak finding function. Specifically, for each signal we implemented the following steps [26]:

- to smooth the signal via the MATLAB's embedded function "*smooth*" with a moving window of 1 s;
- to identify the peaks using "*findpeaks*", a MATLAB's embedded function; to this aim, we computed the temporal threshold for the peak detection by inverting the frequency corresponding to the maximal peak of the signal PSD; conversely, we used the median value of the whole signal in order to define the amplitude threshold;
- to compute $T_R[n]$, defined as the elapsed time between two consecutive peaks.

This allows retrieving information regarding the *RR* variability during each trial. Consequently, we estimated the *RR* for each breath and for each subject ($f[n]$) by calculating $\frac{60}{T_R[n]}$, obtaining $f^{SG}[n]$ and $f^{\varphi}[n]$. To compare the smart garment with the reference flowmeter, we calculated the mean absolute error (*MAE*) as follows:

$$ MAE = \frac{1}{N_{breaths}} \sum_{n=1}^{N_{breaths}} |f^{SG}[n] - f^{\varphi}[n]|, \tag{5} $$

denoting $N_{breaths}$ the total number of breaths for each trial.

To test the agreement with the reference system, we performed a Bland-Altman analysis between $f^{SG}[n]$ and $f^{\varphi}[n]$. We calculated the mean of the differences (MOD) and the limits of agreement (LOA) [39].

VI. Results

A. Sensor Selection

The percentage use of each sensor in each trial (${}^{j}\Omega_i$) is reported in Fig. 3, in which each piezoresistive sensor is represented by a circle with radius proportional to ${}^{j}\Omega_i$ itself. Therefore, larger circles indicate piezoresistive sensors that have been more frequently used along subjects during each single trial. Concerning the *quiet breathing* at rest condition (speed: 0 km·h^{-1}), only S_3 (right lower Thorax) resulted to have a percentage use higher than 50%. Conversely, considering walking speeds from 1.6 km·h^{-1} to 5 km·h^{-1}, S_1 (right upper Thorax), S_3 (right lower Thorax) and S_5 (right Abdomen) were found to have a percentage use higher than 50%. Lastly, when the speed of the trial increased, thus at 6.6 km·h^{-1} and 8 km·h^{-1}, four sensors were used more than the 50% between subjects, *i.e. S1*, *S3*, *S5* and *S6* (left Abdomen). Moreover, the right side resulted to be preferred with respect the left one. Furthermore, according to Fig. 4, the number of

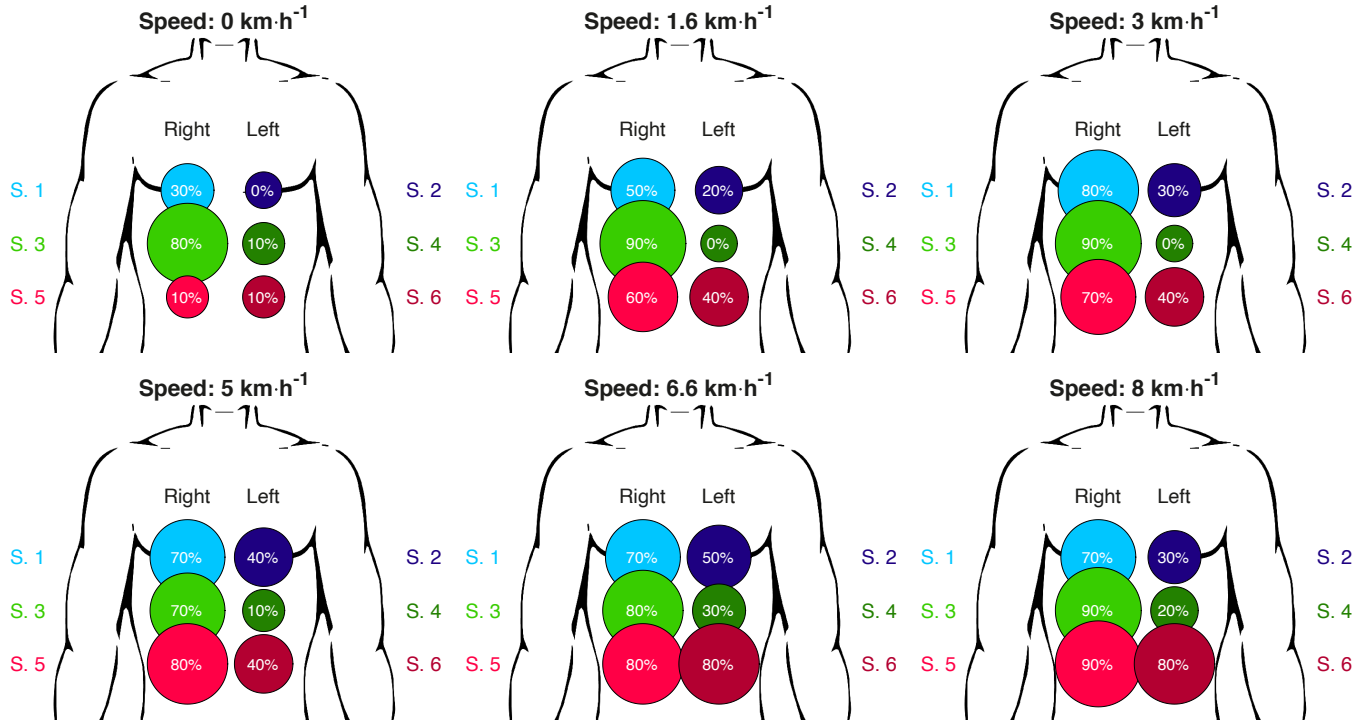

Fig. 3. Percentage use of all sensors over trial speed (${}^{j}\boldsymbol{\Omega}_{i}$, with $i = \{S_1, S_2, S_3, S_4, S_5, S_6\}$). Each sensor is represented as a circle whose radius is proportional to the percentage use. Moreover, to improve readability, in the center of each circle it is reported the specific value of ${}^{j}\boldsymbol{\Omega}_{i}$.

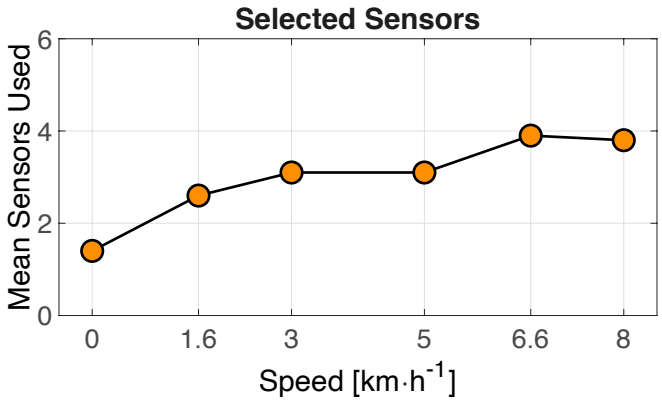

Fig. 4. Number of sensors selected by the proposed algorithm, averaged along subjects. These represent the needed sensors to monitor the *RR* over the speed.

selected sensors increases as the speed of trial increases, except for *S3* that resulted with a percentage use always higher than 70% (see Fig. 3).

Therefore, for monitoring the quiet breathing activity at rest, just one sensor is sufficient. Conversely, when it comes to assess low speed walking, three sensors should be used. Whereas, for high speed walking and running, there is the need of four sensors, placing two of them on both sides of the abdomen and the remaining twos on upper and lower thorax respectively.

The percentage use of each sensor averaged along the trial speeds (Ω_i) is presented in Fig. 5. We marked as most used sensors the ones that met one of the following criteria:

- an average percentage use higher than 50% (see Fig. 5);
- a percentage use higher than 70% at least in one of the six conditions (see Fig. 3).

Therefore, the most used sensors are *S1*, *S3*, *S5* and *S6*, and we named such a configuration as *General Purpose Configuration* (see Fig. 5). Specifically, although *S6* had an average percentage use of 48%, its employment increases with the increasing of the speed, going up to 80% for speeds above 6.6 km·h^{-1} (see Fig. 3); for this reason we opted to include it within the *General Purpose Configuration*. Thus, for a general purpose device required to assess *RR* from quiet breathing at rest to low speed running it is necessary to include: one sensor on the upper thorax, another one on the lower thorax and the last twos on the abdomen.

B. Performance Assessment

1) Average RR Estimation: The results related to $\tilde{F}^{SG}$ for each speed and considering $\boldsymbol{X}^{sel}$, $\boldsymbol{X}^{DT}$ and $\boldsymbol{X}^{GPC}$ are reported in Table I. Specifically, the three methods allowed

TABLE I
$\tilde{\boldsymbol{F}}_{\boldsymbol{h}}^{\boldsymbol{SG}}$ AVERAGED ALONG ALL SUBJECTS, CONSIDERING $\boldsymbol{SG}$ AS $\boldsymbol{X}^{\boldsymbol{sel}}$, $\boldsymbol{X}^{\boldsymbol{DT}}$ AND $\boldsymbol{X}^{\boldsymbol{GPC}}$. ALL RESULTS ARE REPORTED OVER SPEED.

$\boldsymbol{Speed}$ $[\boldsymbol{km \cdot h^{-1}}]$	$\tilde{\boldsymbol{F}}^{\boldsymbol{X}^{sel}}$ $[bpm]$	$\tilde{\boldsymbol{F}}^{\boldsymbol{X}^{DT}}$ $[bpm]$	$\tilde{\boldsymbol{F}}^{\boldsymbol{X}^{GPC}}$ $[bpm]$
0	0.00	0.00	0.00
1.6	0.10	0.20	0.10
3.0	0.40	0.20	0.40
5.0	-3.60	0.70	-8.20
6.6	0.10	0.10	0.10
8.0	0.10	-6.20	0.10

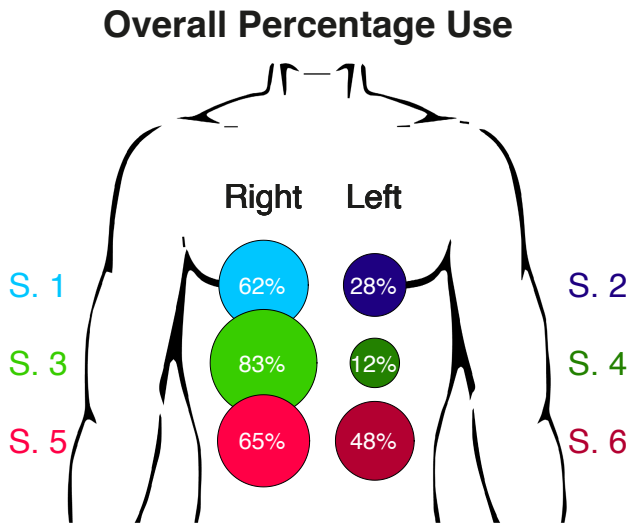

Fig. 5. Percentage use of each sensors averaged along speeds (Ω_i, with $i = \{S_1, S_2, S_3, S_4, S_5, S_6\}$). The configuration composed of *S1*, *S3*, *S5* and *S6* is denoted as *General Purpose Configuration*.

obtaining similar results in terms of $\tilde{F}_h^{SG}$ in each trial:

- considering $\boldsymbol{X}^{sel}$, the estimation of RR was similar to the one estimated using $\boldsymbol{X}^{DT}$ in all trials but one (*i.e.* at speed = 5.0 km·h^{-1})
- the use of $\boldsymbol{X}^{GPC}$ returned good results in terms of $\tilde{F}_h^{SG}$ if compared to the ones obtained considering $\boldsymbol{X}^{DT}$;
- the worst results were obtained at 5 km·h^{-1} in all processing approaches.

For the sake of the completeness, in supplementary material we report the error in estimating the average RR between each selected sensor and the reference flowmeter. We also reported the average breathing rate considering all the volunteers at different speeds.

2) Breath-by-Breath Assessment: The assessment of the different processing methods in terms of MAE are reported in Table II, while the results related to the Bland-Altman analysis are reported in Table III. Moreover, the plots related to the Bland-Altman analysis are reported in Supplementary Materials.

Both the results related to MAE and the output of the Bland-Altman analysis showed comparable results between the three sensor configurations. Moreover, the worst results were obtained at 5.0 km·h^{-1} as previously shown from the Average RR Estimation analysis. This is due to the presence of two outlier subjects for that particular speed, who anyway have not been discarded from the analysis.

VII. Discussion and Conclusions

The present work aims at optimizing the design of wearable systems for respiratory monitoring based on the detection of chest wall movement. Specific attention has been devoted to two crucial aspects on the design of these systems: i) to define the optimal number of sensors and ii) to determine the optimal body location of the sensors. This investigation seeks to provide both guidelines and a general purpose configuration for designing wearables to monitor RR at rest and at different

TABLE II
Results reporting values of $\boldsymbol{MAE}$ over speed for the three sensor configurations.

	$\boldsymbol{MAE}$ $[bpm]$		
Speed $[km \cdot h^{-1}]$	$\boldsymbol{X}^{sel}$	$\boldsymbol{X}^{DT}$	$\boldsymbol{X}^{GPC}$
0.0	0.41	0.46	0.41
1.6	1.17	1.21	1.19
3.0	1.23	1.26	1.44
5.0	1.66	1.74	1.89
6.6	1.34	1.54	1.52
8.0	1.54	1.48	1.48

TABLE III
Results of the Bland-Altman Analysis over speed for the three sensor configurations.

Speed $[km \cdot h^{-1}]$	$\boldsymbol{MOD}$ $[bpm]$	$\boldsymbol{LOA}$ $[bpm]$	$\boldsymbol{N_{breaths}}$
$\boldsymbol{SG \equiv X^{sel}}$			
0	$9.00 \cdot 10^{-3}$	1.18	134
1.6	0.03	3.73	145
3.0	0.01	3.88	135
5.0	0.28	5.76	140
6.6	$-4.00 \cdot 10^{-3}$	4.06	149
8.0	0.14	4.89	142
$\boldsymbol{SG \equiv X^{DT}}$			
0	$5.00 \cdot 10^{-3}$	1.15	134
1.6	0.07	4.05	145
3.0	0.10	3.96	135
5.0	0.35	6.55	140
6.6	0.06	4.66	149
8.0	0.07	4.34	142
$\boldsymbol{SG \equiv X^{GPC}}$			
0	$2.00 \cdot 10^{-3}$	1.12	134
1.6	0.10	3.63	145
3.0	0.18	4.77	135
5.0	0.51	7.35	140
6.6	0.03	4.63	149
8.0	0.08	4.55	142

walking/running speeds. We developed a novel approach for sensory selection based on PCA (see Fig. 2) starting from a custom wearable system equipped with six piezoresistive sensors. We tested the system in ten healthy male volunteers during physical activity performed on a treadmill.

According to previous studies on breathing mechanics during exercise, the quiet breathing at rest mainly involves the pulmonary rib cage. Conversely, with the increasing of the exercise workload, also the abdominal rib cage and the abdomen start increasing their movements [40]. Therefore, we propose the following optimal configuration, in terms both of number of sensors and their body location, depending on the type of activity (Fig. 3 and Fig. 4): at rest just one sensor is sufficient, placed on the lower thorax; during walking the use of three sensors is recommended, placed on upper thorax, lower thorax and abdomen; during running four sensors should be used, *i.e.,* one on the upper thorax, one on the lower thorax, and two on the abdomen.

Another important finding is that sensors belonging to the same band were found to be redundant with respect to each other, only at rest and during walking at low speed; conversely,

at higher speeds both the sensors placed on the abdomen should be used. Indeed, only *S5* and *S6* (i.e., the sensors placed on the abdomen) presented a higher percentage use with the increasing of the trial speed (see Fig. 3). Concerning the selection of more sensors belonging to the right side than to the left one, we reckon that this finding might not be due to any specific characteristic of the human breathing biomechanics in healthy subjects [40]. Rather, it could be likely caused by the specific setup that we prepared for this study. Data clearly show that signals from sensors on the pulmonary and abdominal Rib Cage are redundant in most of the conditions, meaning that they are both providing relevant information even though redundant. In these cases we excluded the sensors with lower weight on principal components, but it is likely that choosing the sensors from the other side would not have affected the results too much. Future studies, will aim to deepen this aspect in order to assess whether the use of one side with respect the other changes the output of the performance analyses.

We also focused on the definition of a general purpose configuration, to assure a correct assessment of RR both at rest and during walking/running. We proposed a 4-sensor configuration which fulfils the two criteria defined in Section VI-A: to select the sensors either with an average percentage use higher than 50% or a percentage use higher than 70% at least in one of the six conditions (see Fig. 3 and Fig. 5).

According to Tables I, II and III, the results, both related to the average RR and the breath-by-breath analysis, were promising and showed similar errors with the ones obtained using a sensor selection method proposed in a previous study [26]. The main advantage produced by our analysis is to obtain similar results just relying on 1 sensor (at rest), 3 sensors (during walking) or 4 sensors (during running) instead of the 6 sensors used in [26]. In addition, the definition of the *General Purpose Configuration* provides a sub-optimal configuration (four sensors) affordable in all the tested scenarios.

It is not easy to compare our results with other studies reporting wearables based on piezoresistive sensors for RR monitoring, since a breath-by-breath analysis for the system under test was not performed or the tests were performed only under one condition (at rest or at one walking speed) or a reference system for monitoring the breathing activity was not used. To the Authors' knowledge, considering both $\boldsymbol{X}^{sel}$ and $\boldsymbol{X}^{GPC}$, the proposed method allowed us to obtain similar results to previous works on the topic. Indeed, concerning the average RR estimation (see Table I), we report values of $\tilde{F}^{SG}$ always below 0.4 bpm (except at 5.0 km·h^{-1}), which is in line with what can be found from similar studies [21], [23], [41], [42]. On the other hand, considering the breath-by-breath estimation, we report values of MOD and LOA always smaller than 0.14 bpm and 4.63 bpm respectively (the condition at 5.0 km·h^{-1} was not considered). Unfortunately, except [26], we did not find any additional study that provided systematic results on breath-by-breath estimation, similar to the one that we implemented in this work.

Summing up, on the basis of the presented results, we suggest the following guidelines:

- for monitoring RR at rest, we suggest to use one piezoresistive sensor placed on the lower thorax. The choice of the side depends on the needs of the experimenter;
- for monitoring RR during low speed walking, we suggest to use three piezoresistive sensors placed on upper thorax, lower thorax and abdomen; again, the choice of the side depends on the needs of the experimenter;
- for monitoring RR during high speed walking or running, we suggest to place four piezoresistive sensors, placing one on the upper thorax, one on the lower thorax and two on both sides of the abdomen;
- for monitoring RR in a general purpose application, we suggest to use the configuration denoted as *General Purpose Configuration* composed of four piezoresistive sensors (see Fig. 5); the main advantage of using this solution is the reduced and fixed number of needed sensors.

In future works, in order to assess the influence of further influencing parameters on the system performance, we will run new experimental sessions to investigate whether the environmental temperature and the activity-related increase of the body temperature might influence the sensor selection. Moreover, we will further develop the smart garment to make it waterproof for increasing the robustness of the system when used in real life scenarios. Furthermore, we will also test the influence of the sweat in order to make the system as reliable as possible when used in unstructured environments. Finally, we will also investigate the possibility to estimate the respiration depth with the proposed system.

The influence of artifacts due to breathing unrelated movements is a crucial point when estimating the RR from rib cage displacements. Considering the wearable device used in this work, it has been already shown that the performance in RR estimation is not significantly affected by torso movements due to walking or low speed running [29], [30]. Moreover, it is worth noting that also the heart pumping activity causes rib cage deformations that are clearly detected by the smart garment during the apnea phase (see supplementary materials for further details). Nonetheless, its influence on the system performance can be considered negligible since they cause signal fluctuations with amplitudes much smaller than the variations caused by breathing. Moreover, we will test the proposed method during different sport activities and employing also different kind of sensors in order to provide comprehensive guidelines in selection the optimal body-location of the sensors for such a purpose.

In conclusion, the proposed analysis may pave the way to future investigations on other fields where the study of the breathing biomechanics could provide useful information. For instance, our techniques could be applied to patients affected by hemiplegia (e.g., due to stroke) [43] or due to lung lobectomy [44]. Indeed, in these patients the asymmetry of breathing biomechanics between left and right side may provide insights regarding respiratory function and how the rehabilitation process is evolving.

REFERENCES

[1] M. A. Cretikos, R. Bellomo, K. Hillman, J. Chen, S. Finfer, and A. Flabouris, "Respiratory rate: the neglected vital sign," *Medical*

Journal of Australia, vol. 188, no. 11, pp. 657–659, 2008.

[2] A. Nicoló, M. Girardi, I. Bazzucchi, F. Felici, and M. Sacchetti, "Respiratory frequency and tidal volume during exercise: differential control and unbalanced interdependence," *Physiological reports*, vol. 6, no. 21, p. e13908, 2018.

[3] F. Q. AL-Khalidi, R. Saatchi, D. Burke, H. Elphick, and S. Tan, "Respiration rate monitoring methods: A review," *Pediatric pulmonology*, vol. 46, no. 6, pp. 523–529, 2011.

[4] C. Massaroni, A. Nicolò, D. Lo Presti, M. Sacchetti, S. Silvestri, and E. Schena, "Contact-based methods for measuring respiratory rate," *Sensors*, vol. 19, no. 4, p. 908, 2019.

[5] H. Liu, Y. Wang, and L. Wang, "A review of non-contact, low-cost physiological information measurement based on photoplethysmographic imaging," in *2012 Annual International Conference of the IEEE Engineering in Medicine and Biology Society*. IEEE, 2012, pp. 2088–2091.

[6] C. Massaroni, D. Lo Presti, D. Formica, S. Silvestri, and E. Schena, "Non-contact monitoring of breathing pattern and respiratory rate via rgb signal measurement," *Sensors*, vol. 19, no. 12, p. 2758, 2019.

[7] C. Massaroni, A. Nicolò, M. Sacchetti, and E. Schena, "Contactless methods for measuring respiratory rate: A review," *IEEE Sensors Journal*, 2020.

[8] C.-T. Huang, C.-L. Shen, C.-F. Tang, and S.-H. Chang, "A wearable yarn-based piezo-resistive sensor," *Sensors and Actuators A: Physical*, vol. 141, no. 2, pp. 396–403, 2008.

[9] S. K. Kundu, S. Kumagai, and M. Sasaki, "A wearable capacitive sensor for monitoring human respiratory rate," *Japanese Journal of Applied Physics*, vol. 52, no. 4S, p. 04CL05, 2013.

[10] D. Wu, L. Wang, Y.-T. Zhang, B.-Y. Huang, B. Wang, S.-J. Lin, and X.-W. Xu, "A wearable respiration monitoring system based on digital respiratory inductive plethysmography," in *2009 Annual International Conference of the IEEE Engineering in Medicine and Biology Society*. IEEE, 2009, pp. 4844–4847.

[11] C. Massaroni, C. Venanzi, A. P. Silvatti, D. Lo Presti, P. Saccomandi, D. Formica, F. Giurazza, M. A. Caponero, and E. Schena, "Smart textile for respiratory monitoring and thoraco-abdominal motion pattern evaluation," *Journal of biophotonics*, vol. 11, no. 5, p. e201700263, 2018.

[12] D. L. Presti, C. Massaroni, J. DAbbraccio, L. Massari, M. Caponero, U. G. Longo, D. Formica, C. M. Oddo, and E. Schena, "Wearable system based on flexible fbg for respiratory and cardiac monitoring," *IEEE Sensors Journal*, vol. 19, no. 17, pp. 7391–7398, 2019.

[13] D. Lo Presti, C. Romano, C. Massaroni, J. DAbbraccio, L. Massari, M. A. Caponero, C. M. Oddo, D. Formica, and E. Schena, "Cardio-respiratory monitoring in archery using a smart textile based on flexible fiber bragg grating sensors," *Sensors*, vol. 19, no. 16, p. 3581, 2019.

[14] V. Balakrishnan, T. Dinh, A. R. M. Foisal, T. Nguyen, H.-P. Phan, D. V. Dao, and N.-T. Nguyen, "Based electronics using graphite and silver nanoparticles for respiration monitoring," *IEEE Sensors Journal*, vol. 19, no. 24, pp. 11 784–11 790, 2019.

[15] T. D. da Costa, M. d. F. F. Vara, C. S. Cristino, T. Z. Zanella, G. N. N. Neto, and P. Nohama, "Breathing monitoring and pattern recognition with wearable sensors," in *Wearable Devices-the Big Wave of Innovation*. IntechOpen, 2019.

[16] G. Aroganam, N. Manivannan, and D. Harrison, "Review on wearable technology sensors used in consumer sport applications," *Sensors*, vol. 19, no. 9, p. 1983, 2019.

[17] N. A. Choudhry, A. Rasheed, S. Ahmad, L. Arnold, and L. Wang, "Design, development and characterization of textile stitch-based piezoresistive sensors for wearable monitoring," *IEEE Sensors Journal*, 2020.

[18] T. Dinh, T. Nguyen, H.-P. Phan, N.-T. Nguyen, D. V. Dao, and J. Bell, "Stretchable respiration sensors: Advanced designs and multifunctional platforms for wearable physiological monitoring," *Biosensors and Bioelectronics*, p. 112460, 2020.

[19] M. Melnykowycz, B. Koll, D. Scharf, and F. Clemens, "Comparison of piezoresistive monofilament polymer sensors," *Sensors*, vol. 14, no. 1, pp. 1278–1294, 2014.

[20] J. Di Tocco, C. Massaroni, L. Raiano, D. Formica, and E. Schena, "A wearable system for respiratory and pace monitoring in running activities: a feasibility study," in *2020 IEEE International Workshop on Metrology for Industry 4.0 & IoT*. IEEE, 2020, pp. 44–48.

[21] A. Lanatà, E. P. Scilingo, E. Nardini, G. Loriga, R. Paradiso, and D. De-Rossi, "Comparative evaluation of susceptibility to motion artifact in different wearable systems for monitoring respiratory rate," *IEEE Transactions on Information Technology in Biomedicine*, vol. 14, no. 2, pp. 378–386, 2009.

[22] Y. Retory, P. Niedzialkowski, C. de Picciotto, M. Bonay, and M. Petitjean, "New respiratory inductive plethysmography (rip) method for evaluating ventilatory adaptation during mild physical activities," *PloS one*, vol. 11, no. 3, p. e0151983, 2016.

[23] M. Chu, T. Nguyen, V. Pandey, Y. Zhou, H. N. Pham, R. Bar-Yoseph, S. Radom-Aizik, R. Jain, D. M. Cooper, and M. Khine, "Respiration rate and volume measurements using wearable strain sensors," *NPJ digital medicine*, vol. 2, no. 1, pp. 1–9, 2019.

[24] A. Fedotov, S. Akulov, and A. Akulova, "Motion artifacts reduction in wearable respiratory monitoring device," in *EMBEC & NBC 2017*. Springer, 2017, pp. 1121–1124.

[25] A. Cesareo, Y. Previtali, E. Biffi, and A. Aliverti, "Assessment of breathing parameters using an inertial measurement unit (imu)-based system," *Sensors*, vol. 19, no. 1, p. 88, 2019.

[26] C. Massaroni, J. Di Tocco, M. Bravi, A. Carnevale, D. L. Presti, R. Sabbadini, S. Miccinilli, S. Sterzi, D. Formica, and E. Schena, "Respiratory monitoring during physical activities with a multi-sensor smart garment and related algorithms," *IEEE Sensors Journal*, 2019.

[27] A. Siqueira, A. F. Spirandeli, R. Moraes, and V. Zarzoso, "Respiratory waveform estimation from multiple accelerometers: An optimal sensor number and placement analysis," *IEEE journal of biomedical and health informatics*, vol. 23, no. 4, pp. 1507–1515, 2018.

[28] L. Raiano, J. D. Tocco, C. Massaroni, G. Di Pino, E. Schena, and D. Formica, "Clean-Breathing: a novel sensor fusion algorithm based on ICA to remove motion artifacts from breathing signal," in *2020 IEEE International Workshop on Metrology for Industry 4.0 & IoT (MetroInd4.0&IoT) (2020 IEEE MetroInd40&IoT)*, Rome, Italy, Jun. 2020.

[29] C. Massaroni, J. Di Tocco, D. L. Presti, E. Schena, F. Bressi, M. Bravi, S. Miccinilli, S. Sterzi, U. G. Longo, A. Berton *et al.*, "Influence of motion artifacts on a smart garment for monitoring respiratory rate," in *2019 IEEE International Symposium on Medical Measurements and Applications (MeMeA)*. IEEE, 2019, pp. 1–6.

[30] C. Massaroni, J. Di Tocco, R. Sabbadini, A. Carnevale, D. L. Presti, E. Schena, L. Raiano, D. Formica, S. Miccinilli, M. Bravi *et al.*, "Influence of torso movements on a multi-sensor garment for respiratory monitoring during walking and running activities," in *2020 IEEE International Instrumentation and Measurement Technology Conference (I2MTC)*. IEEE, 2020, pp. 1–6.

[31] A. Nicoló, C. Massaroni, and L. Passfield, "Respiratory frequency during exercise: the neglected physiological measure," *Frontiers in physiology*, vol. 8, p. 922, 2017.

[32] Shieldex Technik-tex product page. [Online]. Available: https://statex.de/wp-content/uploads/2020/03/ShieldexTechniktexP130B_V.10.pdf

[33] T. A. Wilson, "Mechanics of compartmental models of the chest wall," *Journal of Applied Physiology*, vol. 65, no. 5, pp. 2261–2264, 1988.

[34] Flow sensor spiroquant p by envitec, honeywell. [Online]. Available: https://www.envitec.com/en/products/portfolio/medical-products/flow_sensor_spiroquant_p_ART__E1001117.html

[35] H. Abdi and L. J. Williams, "Principal component analysis," *Wiley interdisciplinary reviews: computational statistics*, vol. 2, no. 4, pp. 433–459, 2010.

[36] I. T. Jolliffe and J. Cadima, "Principal component analysis: a review and recent developments," *Philosophical Transactions of the Royal Society A: Mathematical, Physical and Engineering Sciences*, vol. 374, no. 2065, p. 20150202, 2016.

[37] M. M. Mukaka, "A guide to appropriate use of correlation coefficient in medical research," *Malawi medical journal*, vol. 24, no. 3, pp. 69–71, 2012.

[38] K. E. Barrett, S. M. Barman, S. Boitano, H. L. Brooks *et al.*, "Ganong's review of medical physiology," 2016.

[39] J. M. Bland and D. Altman, "Statistical methods for assessing agreement between two methods of clinical measurement," *The lancet*, vol. 327, no. 8476, pp. 307–310, 1986.

[40] A. Aliverti, "Lung and chest wall mechanics during exercise: effects of expiratory flow limitation," *Respiratory physiology & neurobiology*, vol. 163, no. 1-3, pp. 90–99, 2008.

[41] J. Jeong, Y. Jang, I. Lee, S. Shin, and S. Kim, "Wearable respiratory rate monitoring using piezo-resistive fabric sensor," in *World Congress on Medical Physics and Biomedical Engineering, September 7-12, 2009, Munich, Germany*. Springer, 2009, pp. 282–284.

[42] O. Atalay, W. R. Kennon, and E. Demirok, "Weft-knitted strain sensor for monitoring respiratory rate and its electro-mechanical modeling," *IEEE Sensors Journal*, vol. 15, no. 1, pp. 110–122, 2014.

[43] B. Lanini, R. Bianchi, I. Romagnoli, C. Coli, B. Binazzi, F. Gigliotti, A. Pizzi, A. Grippo, and G. Scano, "Chest wall kinematics in patients

with hemiplegia," *American journal of respiratory and critical care medicine*, vol. 168, no. 1, pp. 109–113, 2003.

[44] A. Cesario, L. Ferri, D. Galetta, F. Pasqua, S. Bonassi, E. Clini, G. Biscione, V. Cardaci, S. Di Toro, A. Zarzana *et al.*, "Post-operative respiratory rehabilitation after lung resection for non-small cell lung cancer," *Lung cancer*, vol. 57, no. 2, pp. 175–180, 2007.

Luigi Raiano received the M.Sc. degree in Biomedical Engineering from the Universitá Campus Bio-Medico di Roma in 2017, where he is currently pursuing the Ph.D. degree.

His research interests focus on the design of wearable mechatronic devices for medical applications.

Joshua Di Tocco received the M.Sc. degree in Biomedical Engineering from Universitá Campus Bio-Medico di Roma in 2018, where he is currently pursuing the Ph.D. degree.

His research interests focus on the design of wearable systems and electronic boards for medical applications.

Carlo Massaroni received the Ph.D. degree in Bioengineering from the Universita' Campus Bio-Medico di Roma (UCBM) in 2016, where he is currently Assistant Professor.

His research interests include the design, development, and test of fiber optic-based sensors and non-invasive techniques to collect physiological parameters.

Giovanni Di Pino received the Medical Degree from Universitá Campus Bio-Medico di Roma in 2003, where he is currently Associate Professor.

His current fields of interest regard clinical neurophysiology and bio-engineering and all the possible matches.

Emiliano Schena received the Ph.D. degree in biomedical engineering from the Universita' Campus Bio-Medico di Roma in 2009, where he is currently Associate Professor.

His main research interests include systems for monitoring physiological parameters, application of fiber optic sensors in medicine, and laser ablation for cancer removal.

Domenico Formica received the Ph.D. degree in bioengineering from the Universita' Campus Bio-Medico di Roma in 2008, where he is currently Associate Professor.

His main research interests lie at the intersection of robotics/mechatronics, neuroscience and developmental psychology.